VOLTAGE-GATED PROTON CHANNEL CONTRIBUTES TO SECONDARY DAMAGE FOLLOWING SPINAL CORD INJURY

By

JIAYING ZHENG

A thesis submitted to the

School of Graduate Studies

Rutgers, The State University of New Jersey

In partial fulfillment of the requirements

For the degree of

Master of Science

Graduate Program in Microbiology and Molecular Genetics

Written under the direction of

Long-Jun Wu, Ph.D

And approved by

_____

_____

_____

New Brunswick, New Jersey

May 2018

ABSTRACT OF THE THESIS

VOLTAGE-GATED PROTON CHANNEL CONTRIBUTES TO SECONDARY

DAMAGE FOLLOWING SPINAL CORD INJURY

by JIAYING ZHENG

Thesis Director: Long-Jun Wu, Ph.D

Traumatic injury to the spinal cord initiates a series of destructive cellular processes that exacerbate tissue damage at and beyond the original site of injury. These processes include oxidative stress responses and pro-inflammatory cascades that can lead to neuronal loss and demyelination of surviving axons. Previous work in our lab has shown that the voltage-gated proton channel Hv1 is necessary for NADPH oxidase-dependent reactive oxygen species (ROS) production by microglia. This means that Hv1 mediated microglial ROS could be a mechanism to cause neuronal damage under disease conditions. Therefore, we hypothesize that Hv1 contributes to ROS production in microglia after SCI, and loss of function can alleviate secondary injury. To test this, we utilized a moderate spinal cord contusive injury model with adult wild-type and $Hv1^{-/-}$ mice, with the aim of studying the role of Hv1 in microglia activation, ROS production, pro-inflammatory response, neuronal cell death, and demyelination. Our results showed that loss of Hv1 reduced microglial activation following spinal cord injury. Moreover, loss of Hv1 alleviated some of the oxidative stress-mediated secondary injury, as well as inflammatory response. $Hv1^{-/-}$ mice

exhibited increased neuronal survival, white matter sparing, and improved locomotive recovery following spinal cord injury. Together, the current study suggested that after spinal cord injury, Hv1 is a potential treatment target to reduce secondary injury.

Acknowledgements

First I would like to acknowledge my thanks to my mentor Dr. Long-Jun Wu, for his unwavering guidance, support, and suggestions throughout my Master's project. His enthusiasm for research and dedicated work attitude always inspire me to follow my research dreams.

I truly appreciate my thesis committee members, Dr. David Axelrod, Dr. Bing Xia, and Dr. Long-Jun Wu, for valuable comments and support during the process of oral presentation and thesis paper revision. It is my first time experiencing this process, and they guide me to think critically and carefully when writing a paper.

I am grateful to my program director Dr. Andrew K. Vershon, for giving me this great opportunity to join the program, and great freedom to choose my courses as well as research lab.

I owe profound gratitude to my project co-worker Dr. Madhuvika Murugan. She is such a well-trained, and organized researcher, as well as a kind, helpful friend. She always patiently taught me how to deal with problems from almost every aspect of research and life.

I am very appreciative to my undergraduate collaborators Miss. Rochelle Mogilevsky, Miss. Peiwen Hu, and Miss. Xin Zheng. We not only helped each other with experiments, but also grew up together.

I highly appreciate the efforts expended by Dr. Dale Bosco and Dr. Ukpong Eyo. They assisted me so much with how to structure my thesis paper as well as its revision ever since I started to write.

I also would like to deeply appreciate Clapham Labs, for providing us the *Hv1*$^{-/-}$

mice.

Last but not the least, I want to express my whole-hearted gratitude to my family,

especially my dear parents. They always encourage me to follow my dreams, and

strongly support me emotionally and financially.

Table of Contents

CHAPTER I: INTRODUCTION

CHAPTER II: VOLTAGE-GATED PROTON CHANNEL CONTRIBUTES TO SECONDARY DAMAGE FOLLOWING SPINAL CORD INJURY

Figures and tables

CHAPTER 1: INTRODUCTION

1.1. Overview of Spinal Cord Injury:

The spinal cord is a critical neural structure connecting the brain and the body. Typically, the spinal cord extends posteriorly from the foramen magnum to the level of the first or second lumbar vertebrae. The spinal cord consists of white matter, nerve fibers with their myelin sheaths, as well as gray matter, consisting mainly of neuronal bodies and branching dendrites. Along the longitudinal axis, spinal cord is divided into cervical region, thoracic region, lumbar region, as well as sacral region.

According to data from the World Health Organization, every year there are approximately 250,000 to 500,000 new spinal cord injury (SCI) cases globally (Bickenbach, Officer et al. 2013). Damage to the spinal cord results in permanent or temporary dysfunction, including loss of muscle control, sensation and neuropathic pain, among other conditions. Either endogenous or exogenous trauma can occur at any region of spinal cord. Traffic accidents, sports injuries, and falls are responsible for most exogenous trauma. Endogenous trauma includes infection, insufficient blood flow and tumors.

Treatments of spinal cord injuries have seen continuous improvement since the middle of the 20th century. Traditional treatments include spine stabilization and inflammation control, while emerging therapies such as stem cell therapy, engineered materials for tissue support, epidural spinal stimulation, and wearable robotic exoskeletons have been rapidly developing. Nevertheless, SCI are incurable in most cases and patients have a much lower quality of life. SCI patients are also two to five times more likely to die prematurely than healthy people. These factors make SCI a

significant concern for not only individuals suffering from the pathology but also for their friends and family making it a serious social burden.

Pathologically, SCI can be separated into primary injury and secondary injury. Primary injury is the initial compression or contusion that results in immediate hemorrhage and cell death at the epicenter (Oyinbo 2011). The primary injury is predominantly not predictable, therefore most research has focused on treatment and prevention of the resulting secondary tissue injury. During secondary injury, neuronal and glial cell disruption results in an enlargement of the injury site, which may further exacerbate clinical symptoms along the rostral-caudal spinal level. In detail, secondary injury can be classified into the sub-acute phase, which happens minutes to weeks after a SCI, and the chronic phase, which can last for years (Oyinbo 2011). (**Table 1.1** summarizes the notable events that happen during each phase).

The sub-acute injury includes a series of oxidative stress responses and pro-inflammation cascades, which can lead to further demyelination of surviving axons, glial scar formation, and additional cell death. The damage that occurs in this sub-acute phase is known to be critical and without therapeutic intervention could lead to permanent deficits. Therefore, this period presents an important window for effective therapeutic intervention (Saghazadeh and Rezaei 2017) and is the focus of current research.

1.2. Overview of Microglial Activation and Polarization

Microglia, as the resident macrophage of the central nervous system (CNS),

reside in the spinal parenchyma and survey the microenvironment for signals of injury or infection, and are one of the first responders to spinal injury (Dibaj, Nadrigny et al. 2010). Under normal conditions, "resting" microglia occupy distinct non-overlapping territories within the CNS and display a highly ramified or branched morphology (**Figure 1.1**). It has been demonstrated that ramified microglia exhibit the feature of surveying their environment by extending and retracting processes (Kierdorf and Prinz 2017). This allows microglia to survey and communicate with neighboring neurons, synapses, and other types of glial cells, and be able to detect and respond to aberrations in the CNS microenvironment.

Upon activation, however, microglia retract processes and increase their soma size, rapidly transforming from a highly ramified morphology to a less branched and amoeboid shape. Similar to macrophages, microglia go through the process which is referred to as polarization which express different functional programs in response to various signals (Hamilton, Zhao et al. 2014). Microglia can be polarized to distinct activation states by anti- and pro-inflammatory cytokines (Cherry, Olschowka et al. 2014). Generally, M2 (anti-inflammatory) microglia is a group of microglia exhibits the feature of downregulating, repairing, or protecting the body from inflammation (Varin and Gordon 2009), while M1 (pro-inflammatory) microglia is a group of microglia aggregating at the injury site, producing various pro-inflammatory cytokines, such as interleukin-6, tumor necrosis factor-α, nitric oxide, interleukin-1β (IL-1β), and reactive oxygen species (ROS) (Tang and Le 2016).

1.3. Overview of Microglia Following SCI

In the context of SCI, M1 microglia are considered to be neurotoxic and growth inhibitory, contributing to glial scaring and pro-inflammatory factors production (Tang and Le 2016). Conversely, M2 microglia facilitate angiogenesis, debris clearance, and enhance the secretion of neurotrophic factors such as insulin-like growth factor 1, promoting neuron survival and axonal regeneration (Kanazawa, Ninomiya et al. 2017). However, the prolonged presence of M2 microglia can also cause excessive fibrotic responses and tissue scarring (David and Kroner 2011, Tang and Le 2016).

During the sub-acute phase, micro-environmental factors favor M1 polarization and dampens M2 polarization (David and Kroner 2011, Tang and Le 2016). The dominant exhibition of M1 microglia producing various pro-inflammatory cytokines may contribute to immune deregulation following the secondary injury (Duris, Splichal et al. 2018). Among these pro-inflammatory factors produced by microglia and other infiltrated leukocytes, reactive oxygen species (ROS) production by NADPH oxidase, which is originally designed as a defense against invading organisms, are largely released and non-selective damage adjacent neurons and glia after SCI. Cells subjected to oxidative stress have increased damaged membrane lipids, cellular proteins, and DNA, and will trigger further calcium-activated proteases and caspase cascades (Andersen 2004, Nathan and Ding 2010). Oxidative stress-mediated secondary injury has been reported as an critical feature in SCI (Jia, Zhu et al. 2012). Therefore, understanding the underlying mechanism of microglial activation and polarization in SCI are critical for treatment in the sub-acute phase.

Specifically, appropriately alleviating oxidative stress response may lead to the development of novel therapeutic approaches for SCI treatment.

1.4. Overview of Voltage-gated Proton Channel, Hv1

ROS include peroxides, superoxide, hydroxyl radical, and singlet oxygen. (Zorov, Juhaszova et al. 2014). In physiological conditions, ROS is necessary for normal cellular redox reactions, as well as, immune responses to eliminate microbial invaders (Jia, Zhu et al. 2012, Zorov, Juhaszova et al. 2014). However, in the context of pathophysiological conditions, excessive production of ROS can exacerbate injury (Kim, Mahapatra et al. 2017). The nicotinamide adenine dinucleotide phosphate (NADPH) oxidase (NOX) family of enzymes is abundantly expressed in phagocytic cells (Chan 2001, Block and Hong 2005). NOX has been demonstrated to be the main source of ROS generation after SCI (von Leden, Yauger et al. 2017). Specifically, phagocytic cells drastically increase oxygen consumption and generate superoxide from membranes-associated NOX (von Leden, Yauger et al. 2017). It has been demonstrated that Apocynin, a potent inhibitor of NADPH oxidase can efficiently alleviate inflammatory responses, cell apoptosis, and loss of motor function after an experimental SCI (Impellizzeri, Mazzon et al. 2011). Similarly, cerium oxide nanoparticles (CONPs), which are effective ROS scavengers, have also been used to suppress inducible nitric oxide synthase (iNOS) activity, efficiently reducing secondary injury (Kim, Mahapatra et al. 2017). It has also been demonstrated that during NOX activation, electrons are transferred across the membrane, which

depolarizes and acidifies microglia (DeCoursey, Morgan et al. 2003).

Both NOX and ROS play critical roles in the pathogenesis of SCI. Therefore, alleviating oxidative stress-related secondary injury is a promising approach to attenuate tissue damage after a SCI. However, most inhibitors for NOX and ROS are non-selective, which may also inhibit normal cellular signaling and other complicated pathways in patients. Therefore it is important to search for a specific target to suppress ROS release from over-reactive immune cells.

In 2006, a mammalian voltage-gated proton channel Hv1 was identified, with the feature of proton efflux in the presence of a proton gradient (Ramsey, Moran et al. 2006). Hv1 is a six-span transmembrane protein, contains voltage-sensing domain and is encoded by the gene *HVCN1* (Ramsey, Moran et al. 2006, Sasaki, Takagi et al. 2006). Hv1 is expressed in various immune cell types, including neutrophils, eosinophils, B lymphocytes, T lymphocytes, macrophages and microglia, and is responsible for the oxidative burst in these cells (Ramsey, Moran et al. 2006, Capasso 2014). The activation of Hv1 is capable of transferring roughly 30,000 protons/channel, the equivalent charge required to balance the activity of ~20 NADPH oxidases (DeCoursey 2003, Okochi, Sasaki et al. 2009, Ramsey, Ruchti et al. 2009, Wu, Wu et al. 2012). The ability of sensing both voltage and pH gradients indicates Hv1 is ideally suited to the task of charge compensation for NOX activation (Wu, Wu et al. 2012).

Within the CNS, under normal conditions, Hv1 is exclusively expressed by microglia. Previous work in our lab showed that Hv1 mediated a robust proton

current and was required for NADPH oxidase-dependent ROS production in mouse brain microglia. Moreover, we found that loss of Hv1 was protective against damage in mice with ischemic stroke (Wu, Wu et al. 2012). The results hint that microglial ROS-related Hv1 function could be a general mechanism causing neuronal damage under disease conditions. Therefore, in this thesis, **we hypothesized that Hv1 was critical in secondary damage after an experimental SCI**. To test this hypothesis, we will use the spinal cord contusion injury model in mice to study the role of spinal microglia/leukocyte Hv1 in microglia activation, ROS production, neuronal cell death and other secondary tissue damage. The current study will be the first attempt to investigate microglia Hv1 function in inflammation and secondary injury in SCI.

FIGURES AND TABLES

Table 1.1- Summary of events in secondary injury

SUB-ACUTE	CHRONIC
Vasospasm	Continued demyelination
Cell death from direct insult	Continued apoptosis
Ischemia	Continued central cavitation
Edema	Glial scar / syrinx formation
Derangements in ionic homeostasis	Alteration of ion channels and receptors
Glutamatergic excitotoxicity	
Plasma membrane compromise / permeability	Regenerative processes, including sprouting by neurons
Free-radical production	Altered neurocircuits
Lipid peroxidation	Syringomyelia
Nitrous oxide excess	
Conduction block	
Excess noradrenaline	
Energy failure and decreased ATP	
Immune cells invasion and release of cytokines	
Inflammatory mediated cell death	
Neurite growth-inhibitory factors	
Central chromatolysis	
Vertebral compression / column	
Demyelination of surviving axons	
Apoptosis	
Initiation of central cavitation	
Astroglial scar launch	

Summary of events in sub-acute phase (left) and chronic phase (right) (Oyinbo 2011).
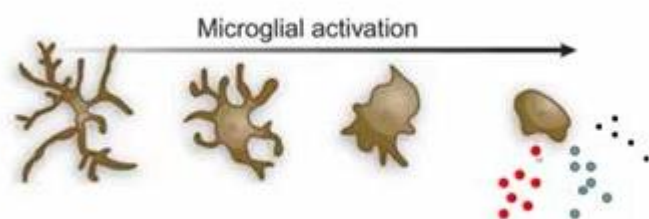
Figure 1.1 Microglia activation.

"Resting" microglia display a highly polarized and ramified shape. After activation, microglia retract processes and increase soma size, and release various cytokines and chemokines.
(https://www.healthrising.org/blog/2015/01/26/getting-younger-leptin-chronic-fatigue -fibromyalgia/microglial-activation-younger/).

CHAPTER 2: VOLTAGE-GATED PROTON CHANNEL CONTRIBUTES TO SECONDARY DAMAGE FOLLOWING SPINAL CORD INJURY

2.1 Materials and Methods:

Animals:

All experiments were conducted in C57BL/6J (Jackson Laboratory, Bar Harbor, Maine) or *Hv1^{-/-}* (Laboratory of David Clapham, Ph.D., Janelia Research Campus) mice 8-10 weeks of age (Ramsey, Ruchti et al. 2009). Both male and female mice were used for studying gender differences, and any deviation is noted in the figure legends. All mice were housed on a 12:12h light:dark cycle with food and water available *ad libitum*. The experiements were performed in accordance with institutional guidelines and approved by the institutional animal care and use committee (IACUC) at Rutgers University.

Moderate contusion model of SCI:

Mice were anesthetized with a mixture of ketamine (60 mg/kg) and xylazine (10 mg/kg) in saline via intraperotoneal (*i.p.*) injection. Anesthetic depth was monitored via toe pinch every 15 mins while surgury was conducted. Laminectomy was performed over the dorsal portion of T10-T9 vertebra. Clamping at T8 and T13 vertabrae to stabilize the spinal column. The exposed dorsal spinal cord was subjected to a 3 g weightdrop with 0.5 mm diameter flat surface tip from a height of 6.25 mm using a modified NYU impactor resulting in a moderate contusion injury (Chen, Kress et al. 2012). After the injury, a small piece of subcutaneous fat was placed on

the dorsal surface before the skin was closed, in order to avoid tissue adhesion between dura and peripheral tissue. For sham control, laminectomy was performed without weight-drop injury.

Locomotion recovery assessment:

Mice were tested for locomotor recovery of the hindlimbs in an open-field chamber starting 2 days after injury and weekly thereafter for up to 8 weeks using the Basso Mouse Scale (BMS) for locomotion (Basso et al., 2006).

Post-surgery Animal Care:

Animals were subcutaneously injected with 0.1 ml 0.125% (50 µl per 25 g body weight of mice) Bupivacaine near the surgical area 5 min after surgery, to provide post-operative analgesia. 0.5 ml Saline (SAL-090; Rocky Mountain Biologicals) and 0.05 ml 20 mg/ml cefazolin (054846; Henry Schein) are subcutaneously injected daily for 3 days. Bladders were manually expressed once daily until reflex bladder function was re-established, usually 7–14 days post-injury. Diet gels were also supplied.

Tissue collection and preparation:

At various timepoints post-injury mice were deeply anesthetized by isoflurane and perfused transcardially with 40 ml PBS followed by 40 ml of cold 4% paraformaldehyde (PFA) in PBS. The spinal cord was removed and post-fixed with 4% PFA for 6 h at 4°C, then transferred to 30% sucrose in PBS overnight. Normally

sample dehrydration in 30% sucrose lasted for 2 days.

Cryosectioning:

Dehrydrated spinal cord tissues were embedded in optimum cutting temperature (O.C.T.) compound and frozen on dry ice. 15 µm thick transverse cryosections were then collected over a 2-4 mm region containing the SCI epicenter with a cryostat (Leica). Sample sections were placed on gelatin-coated glass slides. After drying for 30 min at room temperature slides were stored at -20°C until use.

Immunoflouecentchemistry:

To begin slides were allowed to reaclimate to room temperature for at least 30 mins. Slides were then washed with tris buffered saline (TBS) for 10 min. Blocked slides with 5% goat serum in 0.4% Triton X-100 in TBS for 30-60 min. Then incubated slides overnight with primary antibodies at 4°C. The following primary antibodies were applied for this experiement: rabbit anti-Iba1 (1:500; 019-19741; Wako, Japan); rabbit anti-NeuN (1:1000; AB104225; Abcam); mouse anti-DNA/RNA damage (1:500; AB62623; Abcam, USA); mouse anti-IL-1β (1:300; 12242; Cell Signaling).

After primary antibody incubation slides were re-warmed to room temperature for 30 min and then washed with TBS 3 times for 15 min each wash. Then slices were incubated for 90 min at room temperature with secondary antibody in the dark. The following secondary antibodies used for this experiement: 1:500, Alexa Fluor 594

goat anti-rabbit; 1:500, Alexa Fluor 488 goat anti-mouse; Life Technologies, CA.

Slides were then washed again with TBS. Finally, mounted slides by DAPI

Fluoromount-G (SouthernBiotech, AL).

Quantitative image analysis:

Fluorescent images were captured with a fluorescence microscope (EVOS FL

Cell Imaging System, Life Technologies). ImageJ software (National Institutes of

Health, Bethesda, MD) was applied to cell counting, soma size analysis and

fluorescent signal intensity.

For cell counting, the counted cells were co-localized with the staning with

DAPI. Specifically, for neuron counting, cells double stained by NeuN and DAPI

were considered as cells which survived. NeuN is neuronal marker and DAPI is a dye

binding to AT regions of DNA. After SCI, stained cells labeled by NeuN only could

be cell debris.

For fluorescent signal intensity analysis, we have been aware of the problem

that the measurements of intensity could differ by factors of staining procedures,

antibody concentration, microscope parameters, and image post prosecing. Therefore

all slices were stainined with same procedure and same concentration, imaged with

same parameters (GFP channel, 50% intensity, 250ms, 50% brightness, 33% contrast),

and no photo editing before intensity analysis.

Hematoxylin-eosin (H&E) staining:

Thermo Scientific™ Shandon™ Rapid-Chrome H & E Frozen Section Staining Kit was applied on spinal cord frozen sections (9990001, Thermo Scientific™). Frozen slices were allowed to reacclimate to room temperature for at least 30 mins, and then washed with TBS for 10 min. According to staining protocol, we first placed slides in Rapid-Fixx solution for 5-7 s. Then slices were dipped into distilled water for 10 times. After that, slices were incubated in hematoxylin for 1 min, dipped into distilled water for another 10 times, and dipped 3 times in bluing reagent. Enriched positive charges allowed Hematoxylin to bind DNAs, and turned nucleus into blue by bluing reagent. Slices were then dehydrated in 95% alcohol by 5-7 dips, followed by 15 s Eoxin-Y solution, which stained cytoplasm with red or pink. Finally, slices were dipped 5-7 times into 95% alcohol, 100% alcohol, 100% alcohol again, xylene, and xylene again, in turn, for the purpose of dehydration and clearing.

The slides were analyzed with a light microscope. Grey matter had more densed cells (nucleus) compared to the white matter, thus H&E staining enhanced the contrast between grey and white matter. The perimeter of the white matter was traced and the enclosing area was measured using ImageJ software (National Institutes of Health, Bethesda, MD).

Reactive oxygen species assay:

The reactive oxygen species (ROS) content in whole spinal tissue homogenates was measured using the OxiSelect *in vitro* ROS/RNS assay kit (Cell Biolabs, STA-347) following manufacturer instructions. In brief, mice were perfused transcardially

with 40 ml cold PBS. Approximately16 mg fresh spinal cord samples containing the

SCI epicenter were extracted and homogenized with tissue extraction reagent Ⅰ

(10ml PER 1g of tissue; Invitrogen FNN0071) with protease and phosphatase

inhibitors, and then supernatant was collected after centrifugation. Lysate was added

to the wells along with, dichlorodihydrofluorefscin (DCF), a ROS specific

flurorescent probe in the presence of a catalyst. The resultant fluroescent intensity was

proportional to the amount of free radicals in the sample. The assay was performed in

a 96-well plate format using a standard fluorescence plate reader. By comparison with

the predetermined DCF standard curve, the amount of free radicals in samples was

determined.

Statistical Analysis

All data are presented as the mean ± SEM and were analyzed for significant

differences between groups by Students *t*-test. Significant differences were

determined as $p < 0.05$.

2.3 Results

Mice lacking Hv1 had improved locomotor performance after SCI.

Primary CNS injury is predominantly caused by cell necrosis, which can trigger immune system deregulation following secondary injury (Duris, Splichal et al. 2018). Previous work reported that, in the context of ischemic brain injury, Hv1 contributed to oxidative stress-mediated secondary damage since depletion of Hv1 efficiently reduced the secondary damage (Wu, Wu et al. 2012). Oxidative stress-mediated secondary damage was also reported as one of the key secondary injury mechanisms in SCI (Oyinbo 2011). Therefore, we asked if depletion of Hv1 could reduce oxidative stress-mediated secondary damage within the context of SCI.

To begin, adult wild-type and $Hv1^{-/-}$ mice were subjected to a moderate contusion model of SCI (modified NYU impactor, 3g weightdrop/6.25mm height). Mouse locomotor recovery of the hind limbs was tested in an open-field chamber and recorded according to the Basso mouse scale (BMS) (Basso, Fisher et al. 2006). BMS locomotion testing was performed at regular intervals to trace the progress of recovery (**Figure 2.1**). Successful mouse SCI models resulted in complete motor function loss of the hind limbs 2h after surgery impact (mice score 0, no ankle movement), whereas successful sham surgery models had no effect on hind limb mobility (mice score 9, frequent or consistent plantar stepping, mostly coordinated, paws parallel at initial contact and lift off, and normal trunk stability and tail always up). No significant gender differences were observed (**Figure 2.2**).

BMS locomotion testing started from 2 d post-injury. At 2 d wild-type mice did

not have any motor function recovery, whereas $Hv1^{-/-}$ mice were observed to have slight or extensive ankle movement. One week post-injury, significant mobility function recovery was observed between wild-type (only ankle movement) and $Hv1^{-/-}$ mice (occasional or frequent plantar stepping, no coordination or some coordination). BMS testing was then performed once a week for 8 weeks. The significant recovery differences at early time points persisted even at later time points between wild-type and $Hv1^{-/-}$ mice indicating that Hv1 plays an important role in the secondary damage during the SCI early stage.

Hv1 contributed to microglial activation after SCI.

In the CNS, Hv1 is exclusively expressed on microglial cells. Since we observed significant behavioral differences between wild-type and $Hv1^{-/-}$ mice at early time points, we performed experiments to examine whether $Hv1^{-/-}$ mice exhibits altered microglial activation in the early stage of SCI. Ionized calcium-binding adapter molecule 1 (Iba1) was used to label microglia and monocytes (**Figure 2.3**). In the intact CNS, Iba1 was specially expressed in microglia, yet in injured conditions, the breakdown of blood-spinal cord barrier (BSCB) resulted in the infiltration of monocytes and other immune cells. Microglial number and cell soma size were used to quantify microglial activation (Davis, Salinas-Navarro et al. 2017). In sham condition, no significant microglia density and morphological differences were observed between the two genotypes. After SCI, an increase in the density of Iba1$^+$ cells and cell soma size were observed in both genotypes near the site of injury.

However at 3 d, the microglia soma size in $Hv1^{-/-}$ was smaller compared to that in wild-type mice, and number and soma size of $Hv1^{-/-}$ Iba1$^+$ cells was significantly less than that in wild-types at 7 d (**Figure 2.3**).

Hv1 mediated ROS production after SCI.

Although NOX family NADPH oxidases can transport electrons to reduce oxygen to superoxide for the purpose of host defense, increased NOX activity in the pathological condition can also cause neurodegeneration and other secondary injuries (Bedard and Krause 2007). Previous work reported that microglial NOX2 was responsible for inflammatory neurodegeneration in ischemia stroke, and depletion of Hv1 can efficiently inhibit NOX-mediated damage (Wu, Wu et al. 2012). To test the role of Hv1-mediated ROS in the context of SCI, we used the OxiSelect *in vitro* ROS/RNS assay kit assay to detect the ROS/RNS production in the spinal cord near the site of injury (**Figure 2.4**). ROS/RNS level was low in the sham condition and no significant difference between the two genotypes was observed. At 1 d post SCI, ROS/RNS production in both wild-type and $Hv1^{-/-}$ significantly increased. At 3 d and 7 d post SCI, ROS/RNS production in $Hv1^{-/-}$ mice significantly decreased compared to the WT. This result indicated that and HV1 deficiency results in the reduction of ROS production in the sub-acute injury phase near the site of injury.

Hv1 contributed to inflammation response after SCI.

In biology, inflammatory response results in recruiting immune cells to clean

cellular debris, yet massive necrotic cell death after SCI will cause over-activation of inflammation, which leads to secondary injury cascade (Oyinbo 2011). Recent studies demonstrated that ROS likely function as mediators of microglial activation and contributed to regulate microglia pro-inflammatory responses through MAPKs and NF-κB signal pathways (Bordt and Polster 2014, Park, Min et al. 2015). So far we demonstrated that depletion of Hv1 reduced ROS production, so next we investigated the relationship and effect of reduced ROS on inflammatory response after SCI. Interleukin-1β (IL-1β) was reported to be highly expressed following SCI as determined by RNA sequencing (Zhang, Chen et al. 2014). Also, IL-1β is one of the most well-known pro-inflammatory cytokines aggregating inflammatory response. To investigate IL-1β expression after SCI, we performed immunofluorescence double staining of Iba1 and IL-1β (**Figure 2.5**). By analyzing the IL-1β fluorescent intensity and co-localization with Iba1, we found that microglial expression of IL-1β peaked at 1d and was reduced at later time points following SCI.

Hv1 contributed to motor neuronal death after SCI.

Molecularly, we demonstrated that Hv1 depletion can significantly decrease oxidative stress and pro-inflammation cascades. We then investigated the cellular differences to confirm whether Hv1 depletion reduced the secondary injury. Neuronal survival is one of the most critical measurements of secondary injury. Immunofluorescence staining showed that less neurons survived in the wild-type compared to *Hv1*$^{-/-}$ after SCI (**Figure 2.6**). Further analysis of neuronal survival

showed that compared to the wild-types, neuronal loss was ameliorated in $Hv1^{-/-}$ as

significant differences were observed at 3 d and 7 d of SCI.

Hv1 contributed to demyelination after SCI.

We also investigated tissue damage in addition to neuronal death. By performing

H&E staining, we found the difference in spared white matter between wild-type and

$Hv1^{-/-}$ at 7 d and 28 d following SCI. Spared white matter was reported to be

negatively correlated with glial scarring (Whetstone, Walker et al. 2017). Glial

scarring started approximately at 7 d and matured at 28 d (Hackett and Lee 2016).

Therefore, we picked 7 d and 28 d to investigate the sparing of white matter. H&E

staining enhanced the contrast between grey matter and white matter area. We took

images from epicenter (0 mm, E) and approximately 0.5 mm, 1.0 mm, 1.5 mm away

from directly injured epicenter (both rostral and caudal sites, R1/C1, R2/C2, and

R3/C3, respectively) (**Figure 2.7**). We observed that epicenter exhibited more severe

necrosis, gliosis and white matter loss than the two sides, and injury was more severe

in regions closer to the epicenter than in ones further away. Moreover, at both time

points, there was larger white matter area in $Hv1^{-/-}$ when compared to wild-types. In

addition, less white matter area exhibited in both $Hv1^{-/-}$ and wild-types at 28 d when

compared to 7 d, indicating that the damage to white matter became more severe with

the time. However, the decrease of white matter was less in $Hv1^{-/-}$ when compared to

wild-types from 7 d to 28 d. Together, these results indicated Hv1 depletion

contributed to less secondary damage at both early and longer time points.

Discussion

Hv1 contributed to ROS production following spinal cord injury.

In pathological conditions, excessive reactive oxygen species (ROS) production

contributes to oxidative stress-mediated injury, pro-inflammatory cascades and other

secondary damages. Excessive ROS can take a variety of forms including superoxide,

hydroxyl radicals, nitric oxide, and peroxynitrite. ROS is released from a variety of

sources including cell necrosis, activated resident microglia and infiltrated leukocytes.

Among these sources, NADPH oxidase (NOX), a plasma membrane protein complex,

contributes substantially to ROS generation and is used by the immune system to fight

infections, as well as, mediate inflammatory response within diseased conditions

(Bedard and Krause 2007). NOX generating superoxide requires electrons to transfer

across the membrane, and this will lead to rapid membrane depolarization as well as

cell acidification. Excessive depolarization will inhibit further electron expulsion,

therefore, maintaining the function of NOX requires a charge-compensating

mechanism (DeCoursey 2003). One such mechanism may involve the voltage-gated

proton channel Hv1, which was identified in 2006 (Ramsey, Moran et al. 2006, Sasaki,

Takagi et al. 2006). The highly selective efflux of protons through Hv1 makes it an

ideal candidate for NOX charge compensation (Eder and DeCoursey 2001).

In the current study, we investigated the relationship between ROS production

and depletion of Hv1 following SCI. One day post-SCI, ROS production in both

wild-type and $Hv1^{-/-}$ significantly increased, whereas at days 3 and 7, ROS/RNS

production in $Hv1^{-/-}$ mice significantly decreased when compared to wild-types.

Moreover, the difference in ROS production between wild-type and *Hv1*$^{-/-}$ mice

increased overtime, indicated that 1) proportion of immune cell-generated ROS

increased after SCI 2) Loss of Hv1 down-regulated ROS generation. At 1 day

post-SCI, it is likely that the predominant source of ROS is related to injury induced

necrosis. However, over time, an increased proportion of ROS is generated from

microglia, astrocytes, and infiltrated leukocytes. Together, our result suggest that Hv1

contributes to ROS production during the SCI sub-acute phase.

Loss of Hv1 reduced microglial activation following spinal cord injury.

Microglia are the initial responders to SCI, this is followed by astrocyte

activation and recruitment of the circulating immune cells, such as neutrophils and

macrophages (Popovich, Wei et al. 1997, Taoka, Okajima et al. 1997, Leskovar,

Moriarty et al. 2000). Microglial activation is usually characterized by changes in

morphology, proliferation, and cytokine/chemokine production (Ransohoff and Perry

2009). Under normal conditions, microglia in the spinal cord exhibit a relatively

uniform distribution and density, and are displace typical soma size and ramified

processes. However, upon activation, soma size increases and processes shorten.

When comparing *Hv1*$^{-/-}$ mice to wild-types, these morphological alterations were less

pronounced. This finding is consistent with our lab's previous work in the context of

ischemia stroke, wild-type microglia displayed increased levels of activation as

compared to *Hv1*$^{-/-}$ mice (Wu, Wu et al. 2012). Additionally, Iba1 immunofluorescent

staining on 7 d and 28 d tissue sections revealed fewer reactive microglia within the

lesion site of $Hv1^{-/-}$ mice when compared to wile-types. Together, our result suggested Hv1 contributed to attenuate microglial activation following SCI.

Microglial Activation contributed to ROS-mediated secondary injury

Multiple findings suggested that activated resident microglia and infiltrated leukocytes are important sources of ROS, which contribute to secondary injury following SCI (Bains and Hall 2012, Jia, Zhu et al. 2012).

Previous western blot and electrophysiology results confirmed that in mouse brain tissue, Hv1 was specifically expressed in microglia (Wu, Wu et al. 2012). Proton current was detected in mouse wild-type brain microglia, whereas it was absent in the $Hv1^{-/-}$ mouse brain microglia (Wu, Wu et al. 2012) . Furthermore, previous work showed brain microglia generate ROS through NOX, especially NOX2 (Wu, Wu et al. 2012, Yu, Yu et al. 2017). Hv1 served as a charge-compensation mechanism and pumped H+ to extracellular, which allowed NOX2 to be fully activated (Wu, Wu et al. 2012). Treatment of NOX activator on brain slices showed that the absence of Hv1 caused significant reduction of ROS generation (Wu, Wu et al. 2012). It has been demonstrated that Hv1 was required for NOX-mediated ROS production in brain microglia (Wu, Wu et al. 2012). Absence of Hv1 efficiently reduced microglial ROS production, and resulted in less secondary tissue damage in the context of ischemia stroke (Wu, Wu et al. 2012).

In the current study, we also observed that depletion of Hv1 reduced ROS production after SCI at early time points, and these $Hv1^{-/-}$ mice exhibited earlier and

better functional recovery compared to wild-type mice. Differences were observed at 2 d post-surgery and peaked at 1 week. This indicated that events that occurred at at an early time point were very likely related to microglia because: 1) microglia is an initial responder; 2) Hv1 highly expressed on microglia. Therefore, we performed Iba1 staining to investigate microglial response to SCI. Our staining data showed morphologically, microglia in both wild-type and $Hv1^{-/-}$ mice were highly activated at 1 d and 3 d, but less activated in $Hv1^{-/-}$ mice at 7 d post-surgery. Recent studies pointed out that ROS likely mediated microglial activation (Qin and Crews 2012, Bordt and Polster 2014, Park, Min et al. 2015). Therefore, at 3 d post SCI, although ROS production from microglia was decreased in $Hv1^{-/-}$ mice. The remaining ROS in the environment and generated from other sources may still be able to strongly stimulate microglial activation. Whereas in wild-type mice, microglia activated by ROS may produce more ROS in a positive feedback loop.

Hv1 depletion down-regulated further secondary injury

We further attempted to determine downstream of ROS-mediated secondary injury. ROS can contribute to pro-inflammatory response by activating various kinase, such as c-Jun N-terminal protein kinase, mitogen-activated protein kinase MAPK (p38), as well as signal pathways such as NF-κB pathway (Offen, Gilgun-Sherki et al. 2004, Bordt and Polster 2014, Park, Min et al. 2015). We investigated whether there was difference of IL-1β expression, because: 1) IL-1β was highly expressed in brain microglia (Zhang, Chen et al. 2014); 2) IL-1β up-regulation aggravated secondary

damage (Xu, Tao et al. 2008) 3). IL-1β involved in inflammatory signaling pathways (Akanda, Kim et al. 2018). Our result showed that compared to the wild-types, IL-1β production was less in $Hv1^{-/-}$. Also, the co-localization staining of IL-1β and Iba1$^+$ cells manifested that loss of Hv1 reduced the pro-inflammatory response of microglia and infiltrated monocytes.

Moreover, oxidative stress as well as pro-inflammation may be associated with increasing neuronal damage and death (Hou, Che et al. 2018, Sakamoto, Suzuki et al. 2018). After SCI, survival of remaining neurons and spared white matter were significantly increased in $Hv1^{-/-}$ mice. This indicated that demyelination of surviving axons, and additional neuronal death were associated with oxidative stress responses and pro-inflammation cascades. Eventually, the expansion of the damage could result in the paralysis extending to higher segments (Zhang, Yin et al. 2012). Our mouse locomotion behavior test showed that even after 8 weeks post SCI, wild-types can only do occasional plantar stepping, whereas $Hv1^{-/-}$ mice exhibited consistent plantar stepping and some coordination with front limps. This behavior difference supported that $Hv1^{-/-}$ mice were subjected to less secondary injury.

Together, we reported that Hv1 contributed to oxidative stress mediated-secondary damage and further inflammation following SCI. Depletion of Hv1 can significantly reduce the secondary injury following SCI. Findings from this study may shed light on the possibility of new treatment for SCI by blocking Hv1.

Future Direction:

Generation of conditional microglial Hv1 knockout mice:

It has been well reported that circulating immune cell types such as neutrophils and macrophages can respond to SCI (Popovich, Wei et al. 1997, Taoka, Okajima et al. 1997, Leskovar, Moriarty et al. 2000). These cell types have also been shown to express Hv1 (Schilling, Gratopp et al. 2002, Okochi, Sasaki et al. 2009, Ramsey, Ruchti et al. 2009). Thus, it is likely that neutrophils and macrophages can also play a role in Hv1-mediated ROS damage following SCI. Therefore, we will generate conditional knockouts, CX3CR1$^{creER+/-}$Hv1$^{flox/flox}$, to investigate the microglial contribution alone. CX3C chemokine receptor 1 (CX3CR1) is a specific receptor for the CX3C chemokine, fractalkine (FKN; neurotactin), which is specifically expressed on microglia, monocytes, dendritic cells, as well as subsets of NK cells (Jung, Aliberti et al. 2000). Expression of the tamoxifen-dependent Cre recombinases (CreER) can conditionally delete floxed sequences (Feil, Valtcheva et al. 2009). Therefore, using CX3CR1 expression as a driver, we can conditionally knockout Hv1 in the stated cell types. In addition, our previous work demonstrated that blood borne CX3CR1$^+$ cells turnover on average every 3-weeks, while microglia persist for significantly longer periods of time (Peng, Gu et al. 2016). This difference in replacement rate allows us to have knockout Hv1 expression in microglia but not within other cell types. Using this, we can study specifically microglial Hv1 function in the context of SCI.

Screen potential Hv1 proton channel antagonists:

Hv1 exhibits a feature of mediating outward proton current that results in membrane depolarization and cell acidification. Hv1 activation leads to proton efflux and thus increases intracellular pH (pHi). To detect Hv1 activation, we can load microglia with the pH sensitive dye, BCECF (2 µM), and then acidify microglia via the "rebound acidification" technique. We can then monitor changes to fluorescent intensity over time as intracellular pH (pH_i) recovers. To this end, we will use a compound library containing 10,000 small molecules and test their efficacy in inhibiting pH_i recovery. Potential inhibitors will then be tested for Hv1 proton channel specificity using electrophysiological measurements is a similar manner to Hong *et al.* (2014). Once a suitable candidate is identified, we can examine its effects following SCI. BMS locomotion testing will be used to examine the spinal cord damage in vehicle-treated and candidate Hv1 inhibitor-treated mice.

LITERATURE CITED

Akanda, M. R., I. S. Kim, D. Ahn, H. J. Tae, H. H. Nam, B. K. Choo, K. Kim and B. Y. Park (2018). "Anti-Inflammatory and Gastroprotective Roles of Rabdosia inflexa through Downregulation of Pro-Inflammatory Cytokines and MAPK/NF-kappaB Signaling Pathways." Int J Mol Sci **19**(2).

Andersen, J. K. (2004). "Oxidative stress in neurodegeneration: cause or consequence?" Nat Med **10 Suppl**: S18-25.

Bains, M. and E. D. Hall (2012). "Antioxidant therapies in traumatic brain and spinal cord injury." Biochim Biophys Acta **1822**(5): 675-684.

Basso, D. M., L. C. Fisher, A. J. Anderson, L. B. Jakeman, D. M. McTigue and P. G. Popovich (2006). "Basso Mouse Scale for locomotion detects differences in recovery after spinal cord injury in five common mouse strains." J Neurotrauma **23**(5): 635-659.

Bedard, K. and K. H. Krause (2007). "The NOX family of ROS-generating NADPH oxidases: physiology and pathophysiology." Physiol Rev **87**(1): 245-313.

Bickenbach, J., A. Officer, T. Shakespeare, P. von Groote and W. H. Organization (2013). "International perspectives on spinal cord injury: summary."

Block, M. L. and J. S. Hong (2005). "Microglia and inflammation-mediated neurodegeneration: multiple triggers with a common mechanism." Prog Neurobiol **76**(2): 77-98.

Bordt, E. A. and B. M. Polster (2014). "NADPH oxidase- and mitochondria-derived reactive oxygen species in proinflammatory microglial activation: a bipartisan affair?" Free Radic Biol Med **76**: 34-46.

Capasso, M. (2014). "Regulation of immune responses by proton channels." Immunology **143**(2): 131-137.

Chan, P. H. (2001). "Reactive oxygen radicals in signaling and damage in the ischemic brain." J Cereb Blood Flow Metab **21**(1): 2-14.

Chen, M. J., B. Kress, X. Han, K. Moll, W. Peng, R. R. Ji and M. Nedergaard (2012). "Astrocytic CX43 hemichannels and gap junctions play a crucial role in development of chronic neuropathic pain following spinal cord injury." Glia **60**(11): 1660-1670.

Cherry, J. D., J. A. Olschowka and M. K. O'Banion (2014). "Neuroinflammation and M2 microglia: the good, the bad, and the inflamed." J Neuroinflammation **11**: 98.

David, S. and A. Kroner (2011). "Repertoire of microglial and macrophage responses after spinal cord injury." Nat Rev Neurosci **12**(7): 388-399.

Davis, B. M., M. Salinas-Navarro, M. F. Cordeiro, L. Moons and L. De Groef (2017). "Characterizing microglia activation: a spatial statistics approach to maximize information extraction." Sci Rep **7**(1): 1576.

DeCoursey, T. E. (2003). "Voltage-gated proton channels and other proton transfer pathways." Physiol Rev **83**(2): 475-579.

DeCoursey, T. E., D. Morgan and V. V. Cherny (2003). "The voltage dependence of NADPH oxidase reveals why phagocytes need proton channels." Nature **422**(6931): 531-534.

Dibaj, P., F. Nadrigny, H. Steffens, A. Scheller, J. Hirrlinger, E. D. Schomburg, C.

Neusch and F. Kirchhoff (2010). "NO mediates microglial response to acute spinal cord injury under ATP control in vivo." Glia **58**(9): 1133-1144.

Duris, K., Z. Splichal and M. Jurajda (2018). "The Role of Inflammatory Response in Stroke Associated Programmed Cell Death." Curr Neuropharmacol.

Eder, C. and T. E. DeCoursey (2001). "Voltage-gated proton channels in microglia." Prog Neurobiol **64**(3): 277-305.

Feil, S., N. Valtcheva and R. Feil (2009). "Inducible Cre mice." Methods Mol Biol **530**: 343-363.

Hackett, A. R. and J. K. Lee (2016). "Understanding the NG2 Glial Scar after Spinal Cord Injury." Front Neurol **7**: 199.

Hamilton, T. A., C. Zhao, P. G. Pavicic, Jr. and S. Datta (2014). "Myeloid colony-stimulating factors as regulators of macrophage polarization." Front Immunol **5**: 554.

Hou, L., Y. Che, F. Sun and Q. Wang (2018). "Taurine protects noradrenergic locus coeruleus neurons in a mouse Parkinson's disease model by inhibiting microglial M1 polarization." Amino Acids.

Impellizzeri, D., E. Mazzon, E. Esposito, I. Paterniti, P. Bramanti and S. Cuzzocrea (2011). "Effect of Apocynin, an inhibitor of NADPH oxidase, in the inflammatory process induced by an experimental model of spinal cord injury." Free Radic Res **45**(2): 221-236.

Jia, Z., H. Zhu, J. Li, X. Wang, H. Misra and Y. Li (2012). "Oxidative stress in spinal cord injury and antioxidant-based intervention." Spinal Cord **50**(4): 264-274.

Jung, S., J. Aliberti, P. Graemmel, M. J. Sunshine, G. W. Kreutzberg, A. Sher and D. R. Littman (2000). "Analysis of fractalkine receptor CX(3)CR1 function by targeted deletion and green fluorescent protein reporter gene insertion." Mol Cell Biol **20**(11): 4106-4114.

Kanazawa, M., I. Ninomiya, M. Hatakeyama, T. Takahashi and T. Shimohata (2017). "Microglia and Monocytes/Macrophages Polarization Reveal Novel Therapeutic Mechanism against Stroke." Int J Mol Sci **18**(10).

Kierdorf, K. and M. Prinz (2017). "Microglia in steady state." J Clin Invest **127**(9): 3201-3209.

Kim, J. W., C. Mahapatra, J. Y. Hong, M. S. Kim, K. W. Leong, H. W. Kim and J. K. Hyun (2017). "Functional Recovery of Contused Spinal Cord in Rat with the Injection of Optimal-Dosed Cerium Oxide Nanoparticles." Adv Sci (Weinh) **4**(10): 1700034.

Leskovar, A., L. J. Moriarty, J. J. Turek, I. A. Schoenlein and R. B. Borgens (2000). "The macrophage in acute neural injury: changes in cell numbers over time and levels of cytokine production in mammalian central and peripheral nervous systems." J Exp Biol **203**(Pt 12): 1783-1795.

Nathan, C. and A. Ding (2010). "SnapShot: Reactive Oxygen Intermediates (ROI)." Cell **140**(6): 951-951 e952.

Offen, D., Y. Gilgun-Sherki, Y. Barhum, M. Benhar, L. Grinberg, R. Reich, E. Melamed and D. Atlas (2004). "A low molecular weight copper chelator crosses the blood-brain barrier and attenuates experimental autoimmune encephalomyelitis." J Neurochem **89**(5): 1241-1251.

Okochi, Y., M. Sasaki, H. Iwasaki and Y. Okamura (2009). "Voltage-gated proton channel is expressed on phagosomes." Biochem Biophys Res Commun **382**(2): 274-279.

Oyinbo, C. A. (2011). "Secondary injury mechanisms in traumatic spinal cord injury: a nugget of this multiply cascade." Acta Neurobiol Exp (Wars) **71**(2): 281-299.

Park, J., J. S. Min, B. Kim, U. B. Chae, J. W. Yun, M. S. Choi, I. K. Kong, K. T. Chang and D. S. Lee (2015). "Mitochondrial ROS govern the LPS-induced pro-inflammatory response in microglia cells by regulating MAPK and NF-kappaB pathways." Neurosci Lett **584**: 191-196.

Peng, J., N. Gu, L. Zhou, B. E. U, M. Murugan, W. B. Gan and L. J. Wu (2016). "Microglia and monocytes synergistically promote the transition from acute to chronic pain after nerve injury." Nat Commun **7**: 12029.

Popovich, P. G., P. Wei and B. T. Stokes (1997). "Cellular inflammatory response after spinal cord injury in Sprague-Dawley and Lewis rats." J Comp Neurol **377**(3): 443-464.

Qin, L. and F. T. Crews (2012). "NADPH oxidase and reactive oxygen species contribute to alcohol-induced microglial activation and neurodegeneration." J Neuroinflammation **9**: 5.

Ramsey, I. S., M. M. Moran, J. A. Chong and D. E. Clapham (2006). "A voltage-gated proton-selective channel lacking the pore domain." Nature **440**(7088): 1213-1216.

Ramsey, I. S., E. Ruchti, J. S. Kaczmarek and D. E. Clapham (2009). "Hv1 proton channels are required for high-level NADPH oxidase-dependent superoxide production during the phagocyte respiratory burst." Proc Natl Acad Sci U S A **106**(18): 7642-7647.

Saghazadeh, A. and N. Rezaei (2017). "The role of timing in the treatment of spinal cord injury." Biomed Pharmacother **92**: 128-139.

Sakamoto, K., T. Suzuki, K. Takahashi, T. Koguchi, T. Hirayama, A. Mori, T. Nakahara, H. Nagasawa and K. Ishii (2018). "Iron-chelating agents attenuate NMDA-Induced neuronal injury via reduction of oxidative stress in the rat retina." Exp Eye Res **171**: 30-36.

Sasaki, M., M. Takagi and Y. Okamura (2006). "A voltage sensor-domain protein is a voltage-gated proton channel." Science **312**(5773): 589-592.

Schilling, T., A. Gratopp, T. E. DeCoursey and C. Eder (2002). "Voltage-activated proton currents in human lymphocytes." J Physiol **545**(Pt 1): 93-105.

Tang, Y. and W. Le (2016). "Differential Roles of M1 and M2 Microglia in Neurodegenerative Diseases." Mol Neurobiol **53**(2): 1181-1194.

Taoka, Y., K. Okajima, M. Uchiba, K. Murakami, S. Kushimoto, M. Johno, M. Naruo, H. Okabe and K. Takatsuki (1997). "Role of neutrophils in spinal cord injury in the rat." Neuroscience **79**(4): 1177-1182.

Varin, A. and S. Gordon (2009). "Alternative activation of macrophages: immune function and cellular biology." Immunobiology **214**(7): 630-641.

von Leden, R. E., Y. J. Yauger, G. Khayrullina and K. R. Byrnes (2017). "Central Nervous System Injury and Nicotinamide Adenine Dinucleotide Phosphate Oxidase: Oxidative Stress and Therapeutic Targets." J Neurotrauma **34**(4): 755-764.

Whetstone, W. D., B. Walker, A. Trivedi, S. Lee, L. J. Noble-Haeusslein and J. C. Hsu (2017). "Protease-Activated Receptor-1 Supports Locomotor Recovery by Biased Agonist Activated Protein C after Contusive Spinal Cord Injury." PLoS One **12**(1): e0170512.

Wu, L. J., G. Wu, M. R. Akhavan Sharif, A. Baker, Y. Jia, F. H. Fahey, H. R. Luo, E. P. Feener and D. E. Clapham (2012). "The voltage-gated proton channel Hv1 enhances brain damage from ischemic stroke." Nat Neurosci **15**(4): 565-573.

Xu, J. M., L. J. Tao, D. Fu, Z. P. Lv, L. Li and R. P. Dai (2008). "Activation of interleukin-1 beta (IL-1 beta) signaling in the spinal cord in the rats with experimental cardiac injury." Int J Cardiol **128**(3): 413-418.

Yu, Y., Z. Yu, M. Xie, W. Wang and X. Luo (2017). "Hv1 proton channel facilitates production of ROS and pro-inflammatory cytokines in microglia and enhances oligodendrocyte progenitor cells damage from oxygen-glucose deprivation in vitro." Biochem Biophys Res Commun.

Zhang, N., Y. Yin, S. J. Xu, Y. P. Wu and W. S. Chen (2012). "Inflammation & apoptosis in spinal cord injury." Indian J Med Res **135**: 287-296.

Zhang, Y., K. Chen, S. A. Sloan, M. L. Bennett, A. R. Scholze, S. O'Keeffe, H. P. Phatnani, P. Guarnieri, C. Caneda, N. Ruderisch, S. Deng, S. A. Liddelow, C. Zhang, R. Daneman, T. Maniatis, B. A. Barres and J. Q. Wu (2014). "An RNA-sequencing transcriptome and splicing database of glia, neurons, and vascular cells of the cerebral cortex." J Neurosci **34**(36): 11929-11947.

Zorov, D. B., M. Juhaszova and S. J. Sollott (2014). "Mitochondrial reactive oxygen species (ROS) and ROS-induced ROS release." Physiol Rev **94**(3): 909-950.
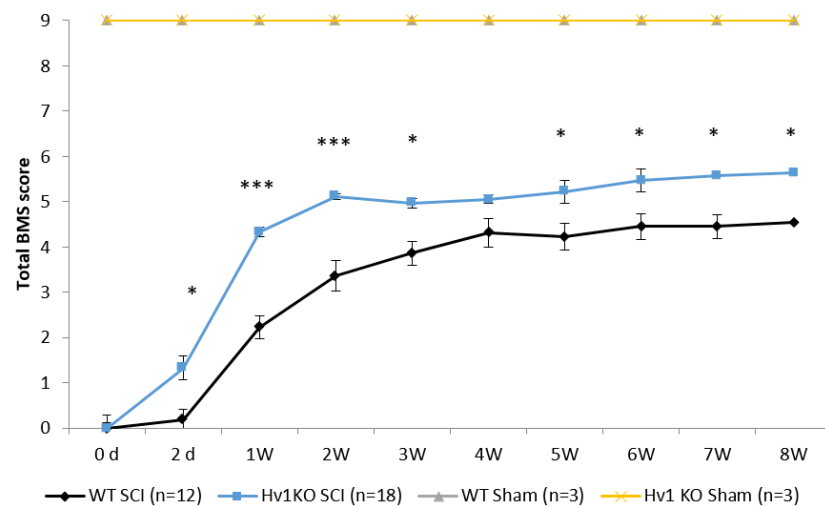
FIGURES AND TABLES

Figure 2.1 *Hv1*^{-/-} **mice display better behavioral performance after SCI compared to the wild-type -** BMS locomotion testing was recorded at regular intervals to trace the progress of recovery (day 0, day 2, week 1 and once a week thereafter for 8 weeks). *Hv1*^{-/-} mice had better BMS scores. All sham wt and *Hv1*^{-/-} had normal scores of 9. (* p<0.05 ***p<0.001, t-test)
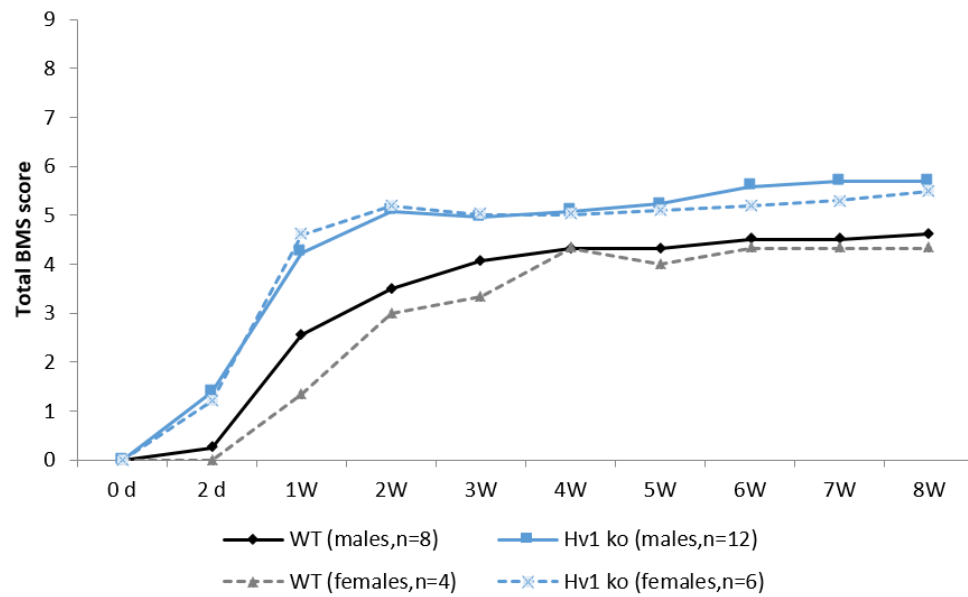
Figure 2.2 No significant gender bias between wt and *Hv1*$^{-/-}$ mice- Total BMS scores were separated into males and females. No significant gender bias observed (p>0.05, wt males vs. wt females; p>0.05, *Hv1*$^{-/-}$ males vs. *Hv1*$^{-/-}$ females; t-test).
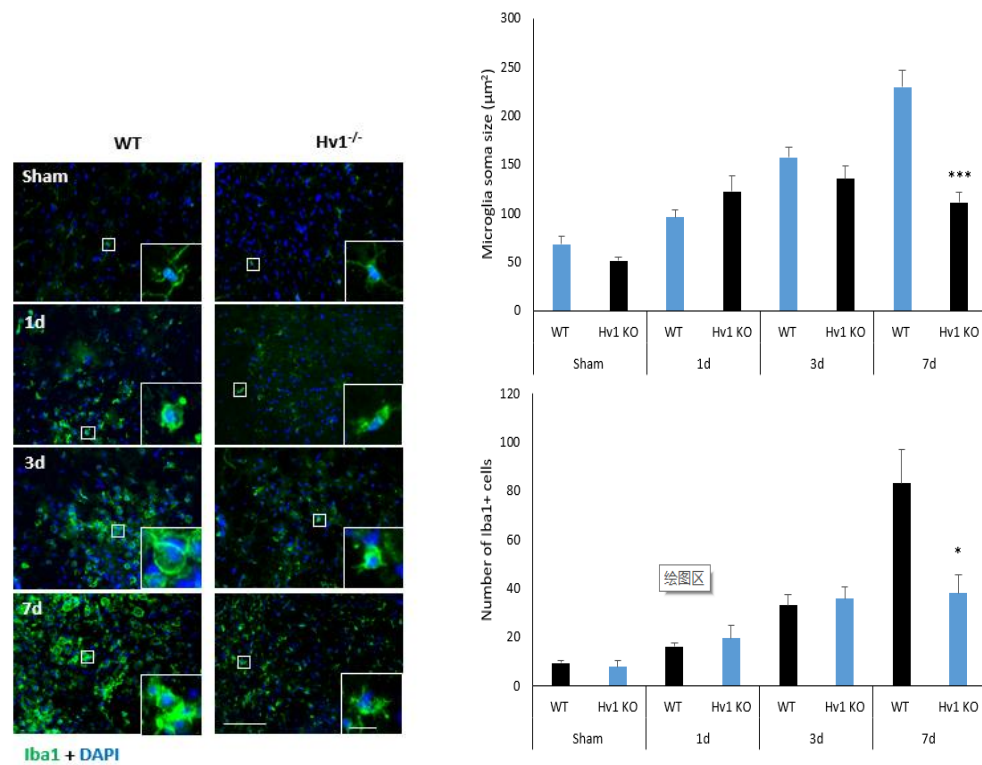
Figure 2.3 Microglial activation in SCI - In SCI, analysis on direct injured epicenter encountered many problems such as severe structural disruption/massive cell necrosis and later glial scares formation. Therefore we picked 1mm away from directly injured epicenter (both caudal and rostral sites) for observation and analysis. $Hv1^{-/-}$ displayed significantly reduced soma size and number of Iba1$^+$ cells at 7 d compared to wt. (n = 3-5 per group, * p<0.05 ***p<0.001 versus wt, SEM as error bars, t-test)
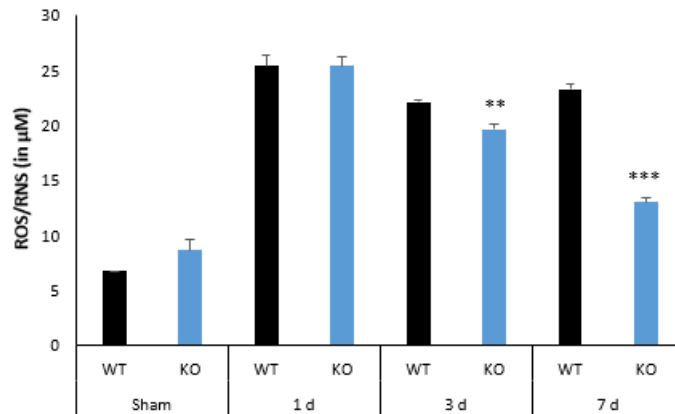
Figure 2.4 ROS/RNS production was less in *Hv1⁻ᐟ⁻* mice - ROS production in wt and *Hv1⁻ᐟ⁻* peaked at 1d and reduced at later time points following SCI. *Hv1⁻ᐟ⁻* displayed significantly less ROS production at 3 d and 7 d compared to wt. (n = 3-5 per group, **p<0.01 ***p<0.001, versus wt, SEM as error bars, t-test)
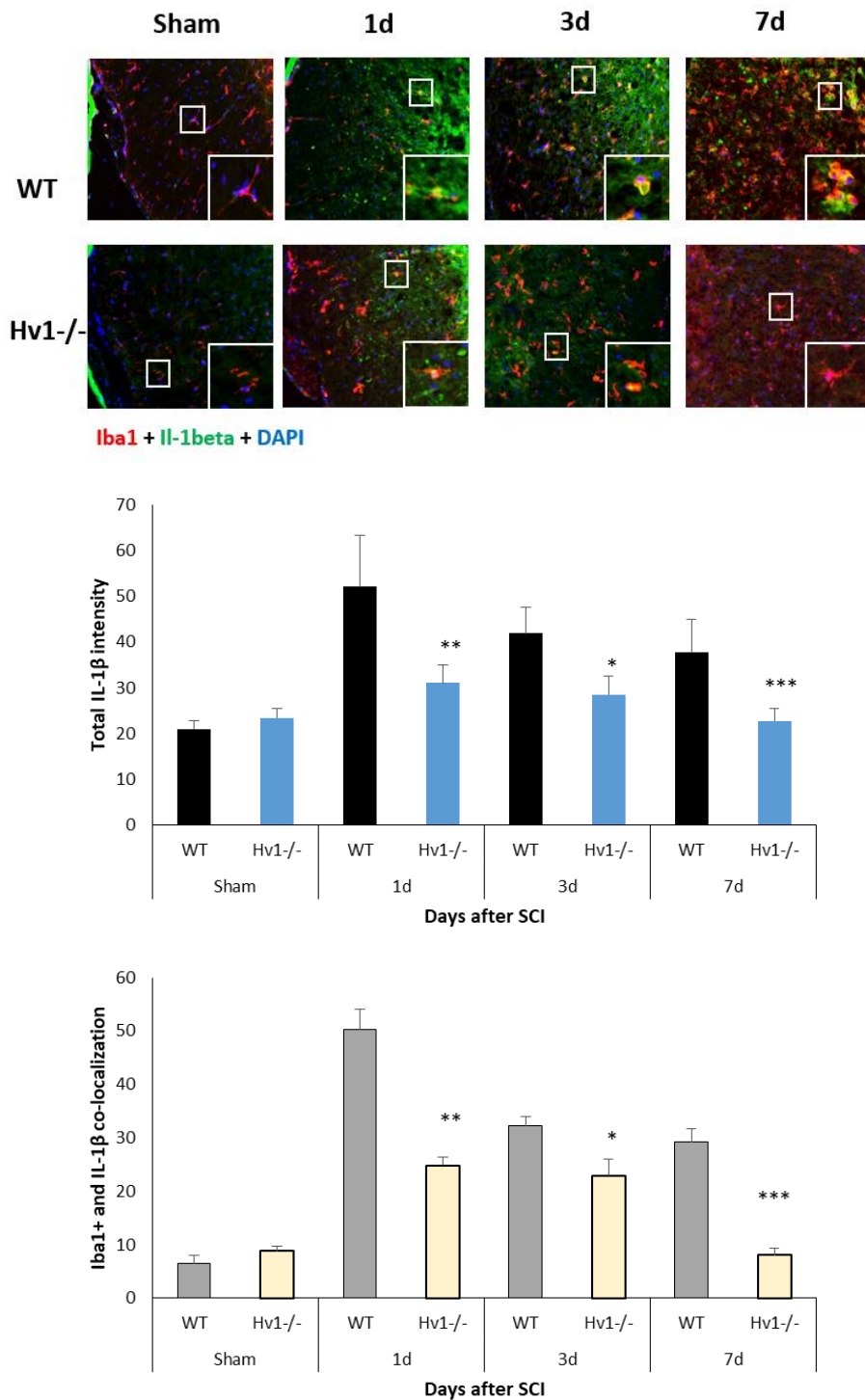
Figure 2.5 Immunofluorescent double staining of Iba1 and IL-1β- The black and blue bars represented total expression of IL-1β, gray and yellow bars represented co-localization of IL-1β and Iba1. Note that expression of IL-1β peaked at 1d and reduced at later time points following SCI. Also, less IL-1β was expressed in Iba1$^+$ cells. (n = 3-5 per group, * p<0.05 **p<0.01 ***p<0.001, versus wt, SEM as error bars, t-test)
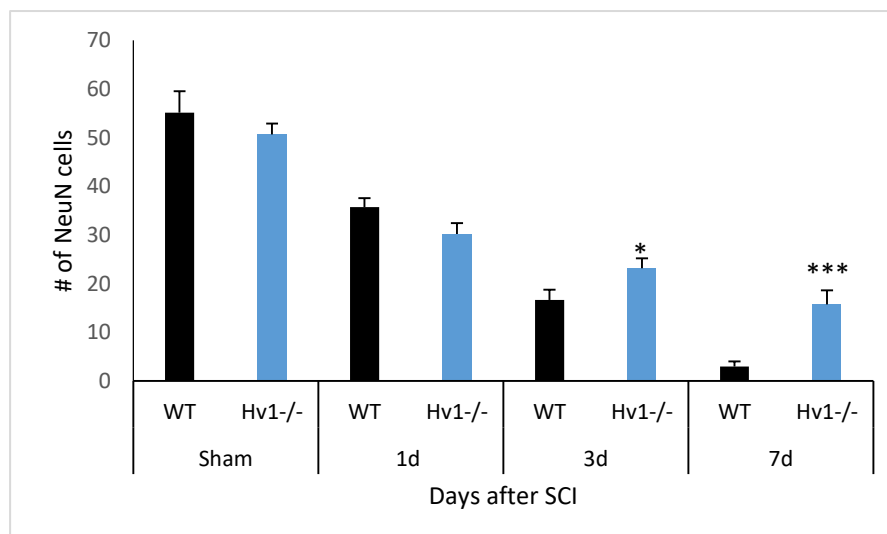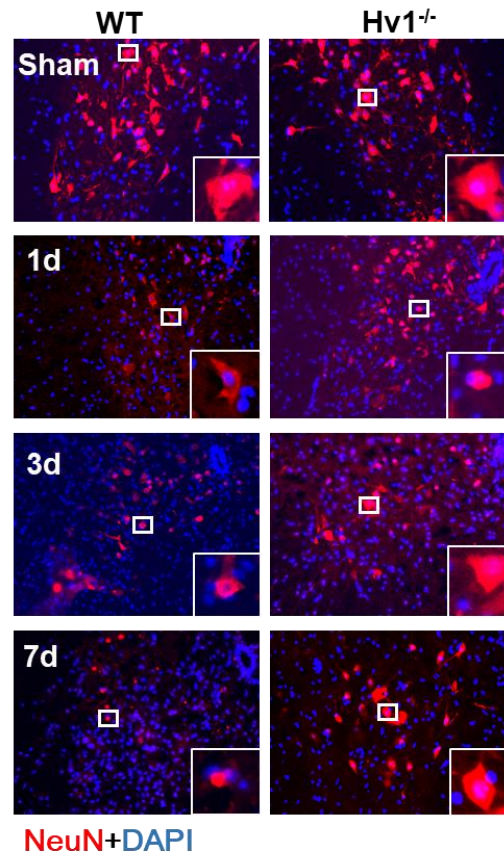
Figure 2.6 Neuronal Survival following SCI- The black and blue bars represented survived neurons in the field of view. Cells double stained by NeuN and DAPI were considered as cells which survived. Cells labeled by NeuN only could be cell debris. Noted that neurons gradually lost after SCI, but more neurons survived in *Hv1*^{-/-} compared to wt at 3 d and 7 d following SCI. (n = 3-5 per group, * p<0.05 ***p<0.001 versus wt, SEM as error bars, t-test)
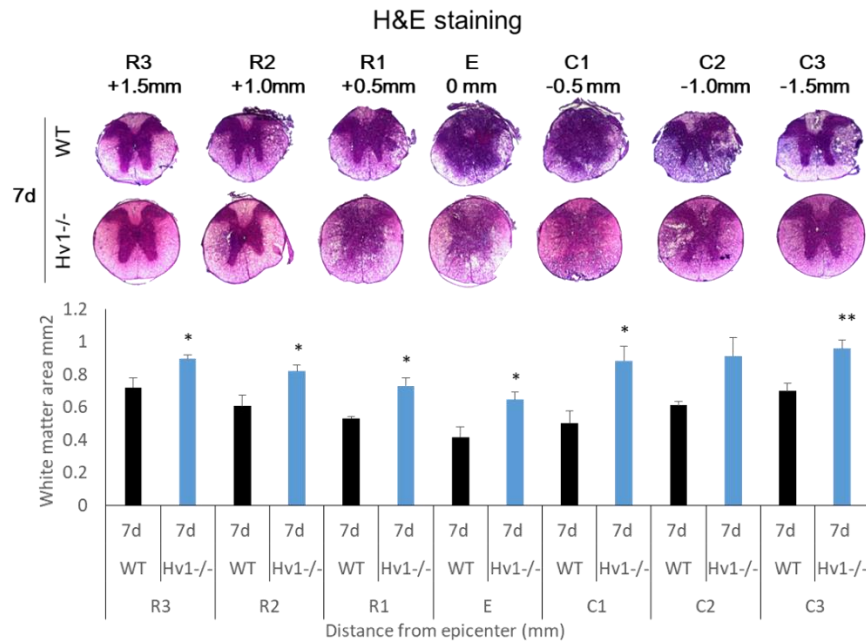
Figure 2.7 White matter sparing following SCI- H&E staining was performed on frozen sections collected from 7 d post SCI mice (wt and $Hv1^{-/-}$). H&E staining can enhance the contrast between grey matter and white matter area. Images were took on epicenter (0 mm, E) and approximately 0.5 mm, 1.0 mm, 1.5 mm away from directly injured epicenter (both rostral and caudal sites, R1/C1, R2/C2, and R3/C3, respectively). White matter area was measured by ImageJ. The black and blue bars represented the white matter area (mm^2) in wt and $Hv1^{-/-}$, respectively. There were more spared matter in $Hv1^{-/-}$ at 7 d when compared to wt. (n = 3-5 per group, * p<0.05 **p<0.01 versus wt, SEM as error bars, t-test)